Available online at www.sciencedirect.com
SCIENCE DIRECT®
Geochimica et Cosmochimica Acta 70 (2006) 711–722
Geochimica
www.elsevier.com/locate/gca

Effect of water on the heat capacity of polymerized aluminosilicate glasses and melts

M. Ali Bouhifd [a,b,*], Alan Whittington [a,c], Jacques Roux [a], Pascal Richet [a]

[a] Physique des Minéraux et des magmas, UMR 7047, Institut de Physique du Globe 4, place Jussieu, 75252 Paris Cedex 05, France
[b] Department of Earth Sciences, Oxford University, Parks Road, Oxford OX1 3PR, UK
[c] Department of Geological Sciences, 101 Geology Building, University of Missouri-Columbia, Columbia, MO 65211, USA

Received 3 May 2005; accepted in revised form 27 September 2005

Abstract

The effect of water on heat capacity has been determined for four series of hydrated synthetic aluminosilicate glasses and supercooled liquids close to albite, phonolite, trachyte, and leucogranite compositions. Heat capacities were measured at atmospheric pressure by differential scanning calorimetry for water contents between 0 and 4.9 wt % from 300 K to about 100 K above the glass transition temperature (T_g). The partial molar heat capacity of water in polymerized aluminosilicate glasses, which can be considered as independent of composition, is $\overline{C}_{p_{H_2O}} = -122.319 + 341.631 \times 10^{-3} T + 63.4426 \times 10^5 / T^2$ (J/mol K). In liquids containing at least 1 wt % H_2O, the partial molar heat capacity of water is about 85 J/mol K. From speciation data, the effects of water as hydroxyl groups and as molecular water have tentatively been estimated, with partial molar heat capacities of 153 ± 18 and 41 ± 14 J/mol K, respectively. In all cases, water strongly increases the configurational heat capacity at T_g and exerts a marked depressing effect on T_g, in close agreement with the results of viscosity experiments on the same series of glasses. Consistent with the Adam and Gibbs theory of relaxation processes, the departure of the viscosity of hydrous melts from Arrhenian variations correlates with the magnitude of configurational heat capacities.

1. Introduction

It has long been known that water exerts a strong influence on the physical and chemical properties of silicate melts and, thus, on phase equilibria, magma ascent, and other petrological and volcanic processes. Thanks to the possibility of making accurate measurements at 1 bar on water-bearing supercooled liquids (Richet et al., 1996), this influence has been recently well documented for the two properties that determine the rate of magma transport, namely, density and viscosity.

As observed for anhydrous melts, the composition and temperature dependences of the density of hydrous melts appear to be rather simple (Ochs and Lange, 1999; Bouhifd et al., 2001). In contrast, the effects of water on viscosity are not only strong, but they depend markedly on melt composition and particularly on water content (e.g., Richet et al., 1996; Dingwell et al., 1996; Davis, 1998; Whittington et al., 2000, 2001, 2004; Romano et al., 2001, 2003). Since viscosity is quantitatively related to configurational entropy through the Adam and Gibbs (1965) theory of relaxation processes (Richet, 1984), knowledge of the heat capacity of hydrous melts should allow useful insights to be derived from these complex variations.

Heat capacity data are lacking for hydrous silicate melts, however. They are very scarce even for hydrous glasses, exceptions being the data of Casey et al. (1976) for SiO_2 with up to 1200 ppm H_2O and of Maschmeyer (1980) for a single silicate glass containing 6 wt % water. As a continuation of our systematic study of hydrous silicate glasses and melts, we report in this paper the heat capacity of four series of hydrous glasses and melts with albite-, phonolite-, trachyte-, and leucogranite-based

* Corresponding author.
E-mail address: alib@earth.ox.ac.uk (M.A. Bouhifd).

0016-7037/$ - see front matter © 2005 Elsevier Inc. All rights reserved.
doi:10.1016/j.gca.2005.09.012

Table 1
Nominal composition[a] of water-free glasses (mol %)

	Albite	Phonolite	Trachyte	DK89
SiO_2	75.30	65.40	69.00	80.25
Al_2O_3	12.07	12.72	10.54	9.93
Na_2O	12.62	10.04	6.95	4.15
K_2O		5.28	2.30	3.43
CaO		2.80	6.15	0.98
MgO		3.10	4.66	0.31
TiO_2		0.66	0.40	0.14
FeO				0.81
gfw (g)[b]	65.381	66.810	64.328	65.513
N[c]	3.242	3.196	3.103	3.178
NBO/T	0.0	0.19	0.21	0.0

[a] Average of a minimum of five analyses made with a Camebax electron microprobe.
[b] Gram formula weight on the basis of one mole of oxides.
[c] Number of atoms per gfw.

compositions (Table 1). Heat capacities were measured by differential scanning calorimetry (DSC) from room temperature up to about 100 K above the glass transition interval: depending on anhydrous bulk composition and water content, the maximum temperature reached ranged from 665 to 1083 K.

These four series were selected to compare the effects of water on volcanologically relevant melts that have similar degrees of polymerization, as characterized by values of nonbridging oxygens per tetrahedrally coordinated cations (NBO/T) between 0 and 0.2, but with different ratios of alkali to alkaline earth elements. These series have already been subjected to viscometry studies (Whittington et al., 2001, 2004) and to determinations of enthalpies of mixing between water and the silicate phase (Richet et al., 2004, 2005), whereas thermal expansion has also been measured for supercooled liquids of the phonolite series (Bouhifd et al., 2001).

2. Experimental methods

The synthesis of the anhydrous samples and hydration techniques have been described in detail by Whittington et al. (2001). Briefly, the anhydrous iron-free glasses were synthesized from oxide and carbonate starting products through repeated cycles of grinding and fusion as described by Schairer and Bowen (1955). The samples were then hydrated at high temperatures at either 2 or 3 kbar in an internally heated vessel with the procedure reported by Whittington et al. (2001) (*cf.* Table 2). At the end of the experiment, the power supply was switched off and the samples were quenched isobarically, with control of the pressure to within 25 bar of the nominal pressure. Typical initial temperature quench rates are 200°/min, with a quench to below 700 K in less than 5 min. Water contents were determined to within ±0.10 wt % by Karl Fischer titration on 10–120 mg samples cut from both ends of each hydrous glass cylinder (Behrens et al., 1996). We measured the room-temperature densities of the glasses by the Archimedean method, using toluene as the immersion liquid (Table 1).

Calorimetric measurements were made with a SETARAM 121 Differential Scanning Calorimeter operated in step-scanning mode. Temperatures were determined from a calibration based on the melting points of indium (429.8 K) and zinc (692.6 K). The calorimetric detector consists of two thermopiles surrounding the sample and reference chambers. Our reference was an empty covered platinum crucible similar to that used for the blank experiments and for the -200 mg samples investigated. Measurements were made at 25° intervals under an argon flow of 15 ml/h. After heating at a rate of 3 K/min, a 600 s hold was made at the final temperature to achieve thermal equilibrium. Measurements were performed in this way up to a maximum temperature of 1100 K in both blank and sample runs. The heat capacity was determined from these observations with the Setsoft SETARAM software. Comparison of the results obtained on pure α-Al_2O_3 and albite and anorthite glasses with reported data for these compositions indicates instrumental inaccuracies of less than 0.4%, and a reproducibility of about 1% (Linard et al., 2001).

The hydrous samples were initially compacted glasses because they had been prepared at a few kilobar pressure (Table 2). Following the same approach as used in dilatometric measurements (Bouhifd et al., 2001), they were first heated from 300 K up to the temperature at which the viscosity is 10^{14} Pa s. Density measurements then showed that the sample had achieved relaxation to the 1-bar density without any weight and water loss (see Richet et al., 2000). A second series of measurements on the relaxed glass was then made and terminated at the same temperature. Possible water loss, which is of special concern in experiments on hydrous samples at atmospheric pressure, could be readily prevented in this way.

Finally, the sample was heated above the glass transition to determine the heat capacity of the supercooled liquid. The experiments were terminated when anomalous heat effects were observed. This happened generally about 100 K above the glass transition, indicating that room-pressure C_p measurements on hydrous liquids are possible over only a narrow temperature interval. These effects and the weight loss measured at the end of these experiment signalled partial crystallization or water exsolution (see Appendix A). That our reported results are nonetheless not beset by these problems is first shown by the intrinsic good reproducibility of the measurements and the overall consistency of the data for the four series of materials investigated. In addition, the molar heat capacity depends primarily on the number of atoms used in the formula weight. Given the relatively high water contents dealt with in this study and the low molar mass of water, any significant water losses would have caused large decreases of the heat capacity, which were not observed.

Table 2
Water contents, gram formula weights, hydration conditions (pressure, temperature and time), and room-temperature densities of hydrated albite, phonolite, trachyte and DK89 glasses

Sample	Water content[a]		gfw (g)	P (kbar)	T (°C)	t (h)	ρ^b (g/cm^3)	ρ^c (g/cm^3)
	wt %	mol %						
Albite								
HAB 0.			65.381					2.371
HAB 0.6	0.67	2.39	64.249	2	1200	65	2.387	2.376
HAB 2.2	1.87	6.47	62.318	2	1200	65	2.375	2.366
HAB 5.2	4.91	15.75	57.920	3	1200	58	2.345	2.335
Phonolite								
Phon 0.			66.810					2.457
Phon 0.5B	0.78	2.83	65.428	2	1200	65	2.472	2.464
Phon 2.2	2.15	7.53	63.135	3	1300	45	2.458	2.450
Phon 5	4.72	15.49	59.251	3	1300	45	2.412	2.406
Trachyte								
Trach 0.			64.328					2.456
Trach 50	0.57	2.01	63.399	2	1200	56	2.477	2.466
Trach 2.2	2.19	7.40	60.901	3	1300	54	2.457	
Trach 5	4.92	15.59	57.121	3	1300	45	2.412	2.398
DK89								
DK89-0.			65.513					2.416
DK89-1.5	1.86	6.45	62.451	2	1200	64	2.346	2.332
DK89-3	3.41	11.36	60.115	3	1200	39	2.336	2.324

[a] Water content measured by Karl-Fischer titration (cf. Whittington et al., 2001, 2004).
[b] Compacted glasses.
[c] Relaxed glasses after DSC measurements.

3. Heat capacity of hydrous glasses

The first measurements were made on glasses synthesized at a few kilobar pressure, which were thus permanently compacted (Richet et al., 2000). During these preliminary measurements up to near the glass transition, the samples relaxed to the 1-bar density. The second series of measurements which were then made are plotted in Figs. 1A–D. The numerical results are listed in Appendix A. They do not differ significantly from the results obtained in the first series, which indicates that the effects of compaction on the heat capacity are within the experimental errors of the measurements.

For the glass phases, we list in Table 3 the coefficients of C_p equations of the form

$$C_p = a + bT + c/T^2, \quad (1)$$

which were least-squares fitted to the experimental data. These data can be compared to values predicted from additive models of calculation from oxide components

$$C_{pg} = \sum x_i \overline{c}_{p_i}, \quad (2)$$

where x_i is the mole fraction and $\overline{c}_{p_i}$ the composition independent partial molar heat capacity of oxide i (Richet, 1987). For the anhydrous endmembers, good agreement is found between such predictions and the experimental data, which are all reproduced to better than 1.5%. These deviations are consistent with the combined uncertainties of the experimental and model values.

For hydrous glasses, the model values can differ by 5% from the experimental data. The reason is that the partial molar heat capacity of water derived by Richet (1987) was from data reported for a single sodium zinc glass (Maschmeyer, 1980) whose reliability and consistency with other data could not be ascertained. We have thus taken advantage of the present observations to derive a new partial molar heat capacity for water by using the coefficients available for all other oxides. The temperature dependence of the partial molar heat capacity of water derived in this way was assumed to be of the Maier–Kelley form (1) as expressions with more adjustable parameters did not improve the quality of the fit. The expression derived is

$$\overline{C}_{p_{H_2O}} = -122.319 + 341.631\ 10^{-3}T + 63.4426\ 10^5/T^2\ (\mathrm{J/mol\ K}). \quad (3)$$

This new equation is valid up to at least 865 K. Along with the partial molar heat capacities of the other oxides, it allows the measurements for all four series of hydrous glasses to be reproduced to within 1% (2σ). Also listed in Table 3 are the average absolute deviations (AAD) of the fitted data from the experimental values. Within a given silicate series, there are no systematic trend for the differences between both kinds of data with increasing water content.

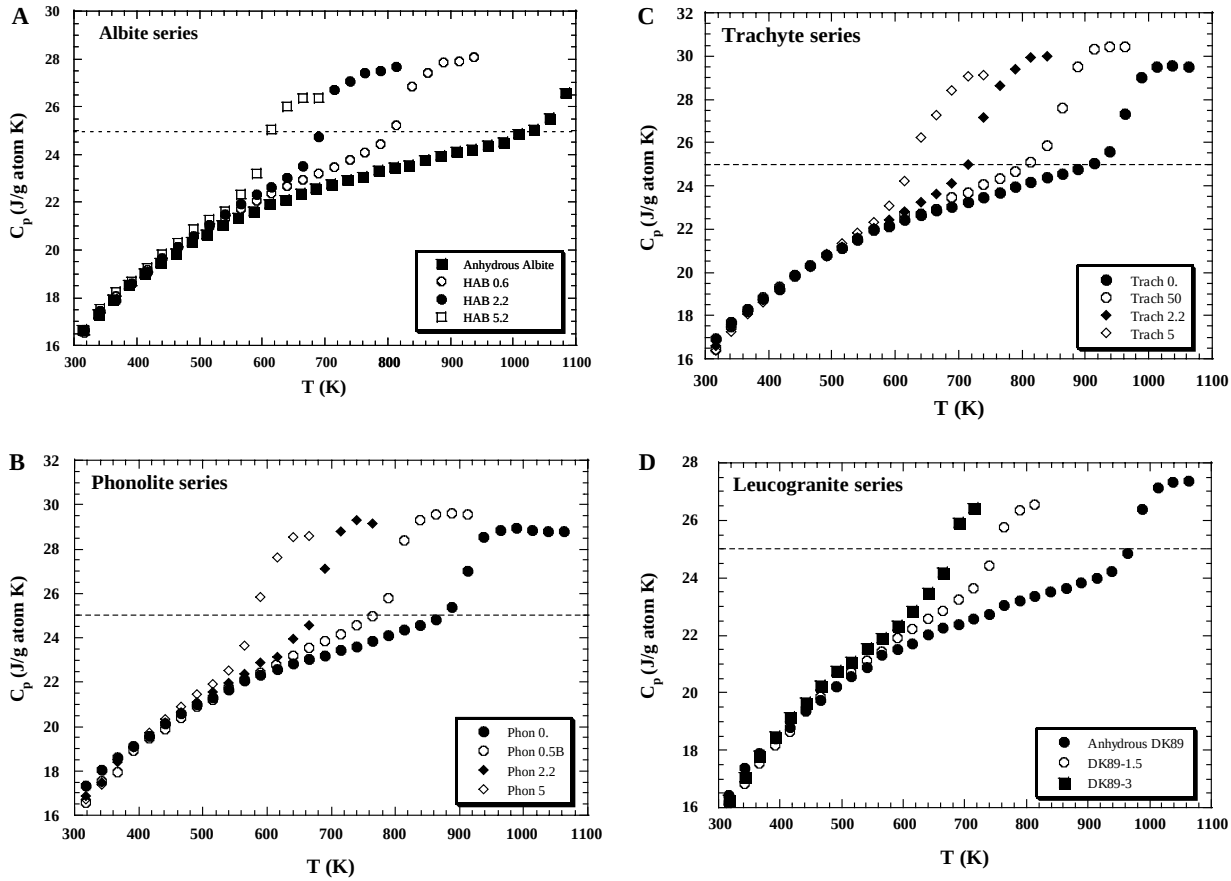

Fig. 1. Heat capacities as measured by differential scanning calorimetry for (A) albite hydrous glasses and melts; (B) phonolite hydrous glasses and melts; (C) Trachyte hydrous glasses and melts; (D) DK89 hydrous glasses and melts. The dashed horizontal lines indicate the Dulong–Petit harmonic limit ($3R$/g atom K).

Table 3
Coefficients of the heat capacity Eq. (1) for hydrous glasses (J/mol K)

	a	$10^3 b$	$10^{-5} c$	ΔT (K)	AAD (%)[a]	N[b]
Albite						
HAB 0.	64.709	17.006	−16.339	300–985	0.25	3.242
HAB 0.6	57.460	29.827	−13.473	300–790	0.22	3.236
HAB 2.2	47.981	44.692	−8.477	300–665	0.20	3.226
HAB 5.2	50.608	41.196	−10.236	300–540	0.29	3.203
Phonolite						
Phon 0.	61.953	22.160	−14.034	300–865	0.31	3.196
Phon 0.5B	54.412	35.356	−12.506	300–765	0.28	3.190
Phon 2.2	53.729	37.841	−12.344	300–615	0.23	3.181
Phon 5	48.875	48.535	−11.492	300–540	0.28	3.165
Trachyte						
Trach 0.	60.555	20.582	−15.095	300–915	0.34	3.103
Trach 50	56.447	27.805	−13.947	300–790	0.34	3.101
Trach 2.2	49.370	38.966	−10.144	300–640	0.14	3.095
Trach 5	46.222	45.356	−9.924	300–565	0.18	3.087
DK89						
DK89-0.	62.292	17.608	−15.940	300–940	0.34	3.178
DK89-1.5	50.966	36.552	−11.694	300–715	0.25	3.166
DK89-3	51.528	38.549	−12.511	300–615	0.20	3.157

[a] Average absolute deviations of the fitted values from the experimental data in the temperature interval ΔT.
[b] Number of atoms per gfw.

4. Heat capacity of hydrous liquids

4.1. Partial molar heat capacity of water

With the exception of titanosilicates and some borosilicates, the heat capacity of liquid silicates is generally constant or increases slightly with temperature (e.g., Richet and Bottinga, 1986; Lange and Navrotsky, 1993; Richet et al., 1997; Tangeman and Lange, 1998; Bouhifd et al., 1998, 1999). The measurements on hydrous phonolite and trachyte melts, which were made over temperature intervals of only 100 K, do not point to strong variations of C_p with temperature. As found for the anhydrous endmembers, we thus assumed that they are constant, at least over not too wide temperature intervals above the glass transition. For extrapolation purposes, one can in fact assume that the C_p–T trends are similar for hydrous and anhydrous liquids for a given compositional series. Owing to a too high glass transition range, the anhydrous albite melt could not be investigated in this study. Because the data for the hydrous melts are consistent with the temperature dependence of the heat capacity determined previously for the dry liquid (Richet and Bottinga, 1984), we also assumed that dC_p/dT is the same for the whole series. As for hydrous DK89 samples, measurements could not be made over wide enough temperatures to determine reliably the heat capacity of the supercooled liquids (cf. Fig. 1D).

These results indicate that the C_p–x_{H_2O} relationship for the hydrous liquids is nonlinear in all series. Water first induces a small but sharp C_p increase before causing a linear decrease at higher contents up to 15 mol % at least (Fig. 2). Because all data refer to relaxed materials, compaction differences between the samples of a given series can be ruled out as a possible explanation for the C_p maximum. Owing to the small number of samples investigated, the position of this maximum is not known precisely although the linear variation observed for $x_{H_2O} > 2$ mol % suggests that it is to be found at concentrations lower than this value, i.e., for water contents lower than about 0.6 wt %.

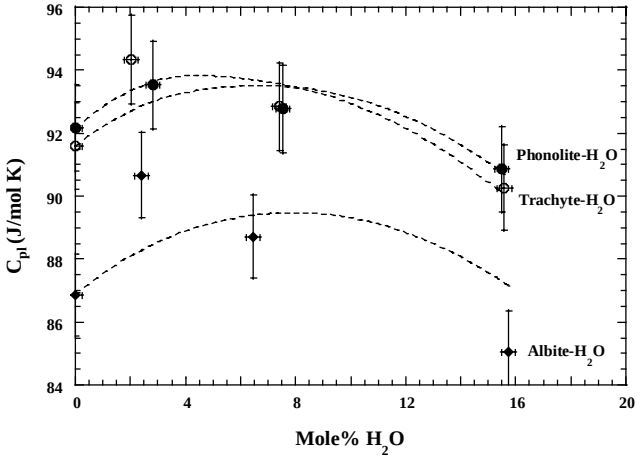

Fig. 2. Heat capacities of hydrous albite, phonolite and trachyte liquids as a function of water content. The dashed lines are the calculated heat capacities for liquids using the calculated individual partial molar heat capacities of OH^- and H_2O_{mol} (see text).

For the anhydrous compositions, the experimental heat capacities of liquids is reproduced to within 2.5% with the model of Richet and Bottinga (1985) for Al-free melts along with the mean $\overline{c_p}$ of Al_2O_3 reported by Courtial and Richet (1993) (see also Bouhifd et al., 1998). To derive the partial molar heat capacity of water from these experiments, the simplest assumption to be checked is whether or not the heat capacity of hydrous silicate liquids is an additive function of composition. Treating the hydrous melt as a pseudobinary mixture of an anhydrous silicate melt and of pure water, one can write

$$C_{pl}^{hyd} = x_{H_2O}\overline{c}_{pH_2O} + (1 - x_{H_2O})C_{pl}^{anh}, \quad (4)$$

where x_{H_2O} is the mole fraction of water, $\overline{c}_{pH_2O}$ the partial molar heat capacity of water, and where the superscripts anh and hyd refer to anhydrous and hydrous melts.

Using the combined data sets for the albite, phonolite, and trachyte hydrous melts, we have obtained 85 J/mol K as the partial molar heat capacity for water in silicate melts. This value is consistent with the large 78–87 J/mol K range derived by Burnham and Davis (1974) and Clemens and Navrotsky (1987) from enthalpies of mixing in the system $NaAlSi_3O_8 \cdot H_2O$, and is higher than the 75 J/mol K heat capacity of pure water. Our result is valid at least up to 965 K, the highest temperature at which C_p data for hydrous supercooled liquids were obtained. With this new value of the partial heat capacity of water and the model of calculation of Courtial and Richet (1993) the experimental heat capacity of hydrous albite, phonolite, and trachyte liquids are reproduced to within 3%. That a constant value accounts, to a first approximation, for all the results suggests that the partial molar heat capacity of water is not strongly dependent on aluminosilicate composition, at least for the range of hydrous melts studied.

4.2. The influence of water speciation

The nonlinear variation of C_p with water content might be related to the dependence of speciation on total water concentration as it is well known that dissolution takes place as either hydroxyl groups or molecular water. At water contents lower than about 3 wt %, hydroxyl groups are the dominant species. Similar abundances of OH^- and H_2O are then found for water contents of 3–4 wt %, whereas molecular H_2O predominates above about 4 wt % (e.g., Stolper, 1982; Silver et al., 1990). This also holds true for the present melts (Figs. 3A and B; Whittington, Withers, Behrens and Richet, unpublished data). In particular, there is good agreement between our infrared spectroscopy data and those for a natural (iron-bearing) phonolite composition (Carroll and Blank, 1997). Combining the experimental heat capacity and water speciation

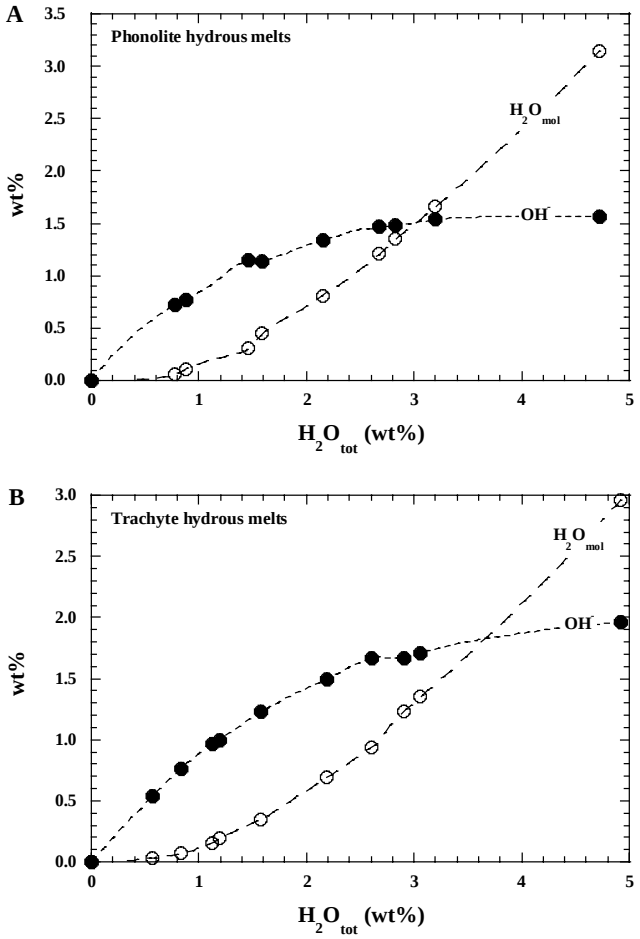

Fig. 3. Speciation of water in the quenched hydrous glasses as determined from infrared spectroscopy measurements on hydrous phonolite samples (A) and on hydrous trachyte samples (B).

data, we thus derived separate $\overline{c_p}$ values for water dissolved as hydroxyl groups and as molecular water. For this purpose, we calculated the concentrations of dissociated and molecular water by using our own speciation data for phonolite and trachyte, and those of Silver and Stolper (1989) for albite, the mole fraction of water dissolved as hydroxyl ions being defined here as the difference between the mole fractions of total and molecular water. In this way, we found that the partial molar heat capacity of water in the form of OH^- ions is 153 ± 18 J/mol K, whereas that of molecular water is 41 ± 14 J/mol K. However, the agreement of model values with experimental data is not as good with these separate partial molar values as with the single value of 85 J/mol for total water so that the latter should be used for thermochemical calculations. The reason could be that water speciation is typically measured on quenched glasses even though the OH^-/H_2O ratio increases with increasing temperature above the glass transition (Nowak and Behrens, 1995; Shen and Keppler, 1995; Sowerby and Keppler, 1999; Behrens and Nowak, 2003). Hence, the variation of the OH^-/H_2O ratio should not be neglected when calculating the partial molar heat capacity of OH^- and H_2O.

5. Glass transition

For all samples, an abrupt C_p change separates the glass from the supercooled liquid. The glass transition temperatures (T_g) listed in Table 4 are given by $(T_A + T_B)/2$, where A and B are the intersections between the C_p line tangent to the data at the inflexion point, in the glass transition range, and the C_p curves of the glasses and supercooled liquids,

Table 4
Calorimetric and viscosity glass transition temperatures, heat capacites of hydrous glasses at T_g, heat capacities of liquids, C_{pl} $(T) = a + bT$, and configurational heat capacities and C_p increases at T_g

	T_{gDSC}	T_{12}	C_{pg} (T_g)	a	10^3 b	C_p^{conf} (T_g)	ΔC_p (%)
Albite							
HAB 0.	1096[a]	—	81.99	75.167[a]	10.655[a]	4.85	5.9
HAB 0.6	815	—	79.74	80.406	10.655	9.35	11.7
HAB 2.2	690	712	77.04	80.143	10.655	10.45	13.6
HAB 5.2	602	—	72.58	76.997	10.655	10.83	14.9
Phonolite							
Phon 0.	915	919	80.55	92.23	0	11.68	14.5
Phon 0.5B	802	—	80.82	94.41	0	13.59	16.8
Phon 2.2	690	684	77.25	92.92	0	15.67	20.3
Phon 5	592	596	74.33	90.39	0	16.06	21.6
Trachyte							
Trach 0.	965	971	78.80	91.59	0	12.79	16.2
Trach 50	865	883	78.63	94.22	0	15.59	19.8
Trach 2.2	740	733	76.35	92.71	0	16.36	21.4
Trach 5	640	628	72.83	89.80	0	17.07	23.4
DK89							
DK89-0.	975	990	77.78	86.71	0	8.93	11.5
DK89-1.5	750	758	76.25				
DK89-3	678	687	74.94				

Data in K and J/mol K.
[a] From Richet and Bottinga (1984).

respectively. This procedure is similar to that described by Moynihan (1995) to determine the limiting fictive temperature of melts (see also Toplis et al., 2001). The method we used to determine the calorimetric T_g is shown graphically in Fig. 4. For convenience, we list in Table 4 the heat capacities of glasses and supercooled liquids at the calorimetric T_g along with the C_p increases and the configurational heat capacities $\left(C_p^{conf}\right)$ at the glass transition.

Operationally, the glass transition temperature is defined as the temperature at which the viscosity is 10^{12} Pa s. Because the viscosity of nearly all our samples has been previously determined (Whittington et al., 2001, 2004), this definition may be quantitatively assessed. The viscosity of these materials is indeed $10^{12.2\pm0.4}$ Pa s at the calorimetric glass transition temperatures. Consistent with the close connection between viscosity and glass transition, these variations parallel (Fig. 5) those observed for the temperature of the 10^{12} Pa s viscosity isokoms as determined from the equations given by Whittington et al. (2001, 2004). The good agreement demonstrates the validity of our method to determine the calorimetric T_g. More important, it also indicates that the similarity of relaxation kinetics for enthalpy and viscosity (e.g., Webb and Knoche, 1996; Sipp and Richet, 2002) holds true for hydrous melts.

For the albite, phonolite, trachyte, and DK89 series, water strongly decreases the glass transition temperature, especially at the low contents where it mostly dissolves as hydroxyl ions. For example, addition of only 1 wt % H_2O reduces the glass transition temperature from 1020 to 850 K for albite, from 915 to 790 K for phonolite, and from 965 to 820 K for trachyte melts, whereas an additional 1 wt % (to 2 wt % H_2O total) causes smaller decreases to 690 and 740 K for phonolite and trachyte melts, respectively. We have reported in Fig. 6 the effect of water on the glass transition temperatures in terms of $\Delta T_g = (T_g^{hyd} - T_g^{anh})/T_g^{anh}$, where T_g^{anh} and T_g^{hyd} are the glass transition temperatures of the anhydrous and hydrated glasses, respectively. This figure shows that the effect of water is more pronounced for albite (NBO/$T = 0$), which is the more polymerized melt, than for phonolite (NBO/$T = 0.19$) or trachyte (NBO/$T = 0.21$). These results may therefore indicate that the effect of water on the glass transition is strong enough that T_g can be used, to a first approximation, as a probe of hydrous silicate melt structure. The exception is the leucogranite DK89 (NBO/$T = 0$) series for which the observed trend differs from that of albite melts and is the same as for phonolite and trachyte melts. This specificity may indicate that the DK89 composition contains some nonbridging oxygens. In fact, the calculated values of NBO/T should be treated only as a guideline, because nominally fully polymerized compositions can contain some nonbridging oxygens (Toplis et al., 1997, 2000; Stebbins and Xu, 1997).

Alternatively, the less dramatic effect of water on T_g (and viscosity) for the leucogranite, as compared to albite, could be related to its more complex composition.

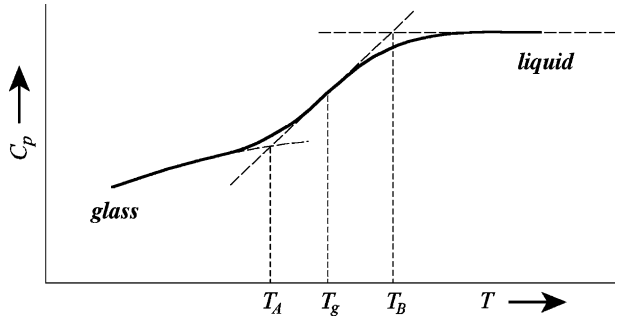

Fig. 4. Schematic diagram illustrating the procedure used for determining the calorimetric glass transition temperature (Linard, 2000).

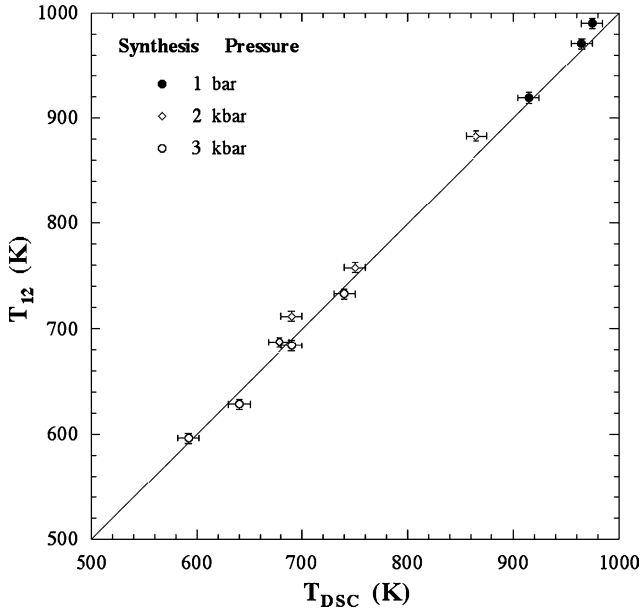

Fig. 5. Comparison of glass transition temperatures as determined from DSC and viscosity experiments, demonstrating that the thermal effects of sample synthesis have been erased completely prior to determination of the calorimetric glass transition.

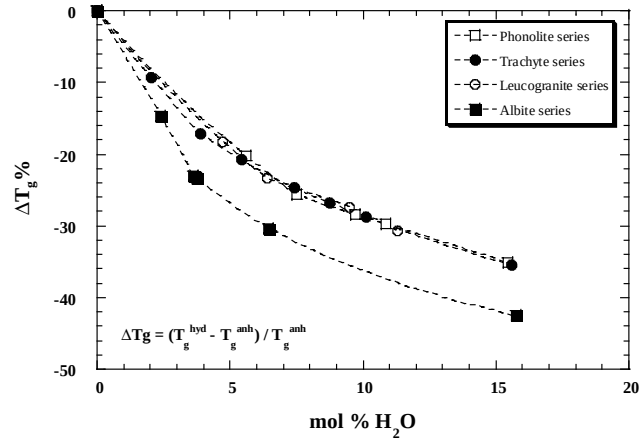

Fig. 6. Effect of water on the glass transition temperature for albite (NBO/T = 0), phonolite (NBO/T = 0.19), trachyte (NBO/T = 0.21) and DK89 (NBO/T = 0) samples, expressed as $\Delta T_g = \left(T_g^{hyd} - T_g^{anh}\right)/T_g^{anh}$.

Whittington et al. (2004) noted that addition of water should result in higher entropies of mixing in simple model compositions than in complex natural melts. Because these entropies of mixing contribute to the configurational entropy of hydrous liquids, they can cause dramatic viscosity reductions (and decreases in T_g) for simple systems with even small amounts of dissolved water. This confirms that simple approximations of the degree of polymerization of the melt structure, such as NBO/T, are just starting points for detailed modelling of the thermodynamics and physical properties of silicate melts.

6. Configurational heat capacity of hydrous melts

The glass transition of silicates usually takes place when the heat capacity becomes close to the Dulong and Petit harmonic limit of $3R$/g atom, where R is the gas constant (Haggerty et al., 1968; Richet and Bottinga, 1986). Despite significant differences in bond strength when the composition varies, silicates thus undergo the glass transition when the Dulong and Petit limit has been reached for all modes of vibration. The anhydrous glasses conform to this rule, but not the hydrous materials for which $C_{pg}(T_g)$ regularly decreases when the water content increases. The effect is small, but significant and systematic (Fig. 7). For samples containing about 5 wt % H_2O (~15 mol % H_2O), the glass transition takes place when C_p is only 93% of the Dulong–Petit limit for phonolite and trachyte, and about 91% for albite hydrous melts.

Similar effects have been observed for borosilicates (Richet et al., 1997), the extreme case being that of pure B_2O_3 for which $C_{pg}(T_g)$ is only 60% of $3R$/g atom K as noted by Haggerty et al. (1968). In both cases, these features point to the existence of weaker elements in the structure, which allows the onset of cooperative configurational rearrangements to take place with lower thermal energy. For hydrous melts, it is tempting to associate such elements with weak hydrogen bonds whose relevance is also indicated by compressibility and volume data (Richet and Polian, 1998; Richet et al., 2000).

This anomaly has interesting implications regarding transport properties because it contributes to the regular increase, from about 6% to 23%, of the C_p change at the glass transition observed in all series when the water content increases (Fig. 8). Since the lack of compositional effects on the heat capacity is a salient feature of glasses just below the glass transition, the complexities affecting melts find their roots in the structural changes that begin to take place at this transition. The thermodynamic measure of these changes is given by the configurational heat capacity, which represents the energy needed, not to increase the temperature, but to achieve a new equilibrium configuration when the temperature is varied. It is given by the difference between the measured C_p and the vibrational heat capacity of the liquid. For silicates, including the hydrous melts investigated here, the great simplifying feature is that the latter can be assumed not to vary significantly above the glass transition temperature (Richet and Bottinga, 1986). For liquid silicates, it is given by

$$C_p^{conf}(T) = C_{pl}(T) - C_{pg}(T_g), \tag{5}$$

where $C_{pl}(T)$ is the C_p of the liquid at temperature T and $C_{pg}(T_g)$ is the heat capacity of the glass at the glass transition temperature.

Within the framework of Adam and Gibbs (1965) theory, melt fragility is related to the temperature dependence of configurational entropy, which is itself determined by the magnitude of the configurational heat capacity (Richet, 1984). The increase in $C_p^{conf}(T_g)$ caused by water in albite, phonolite, and trachyte melts observed in our DSC measurements is thus consistent with the increases in their fragility determined by viscosity measurements (Whittington et al., 2000; Whittington et al., 2004).

The water speciation reaction may be written as

$$H_2O_{mol} + O_b^{2-} = 2OH^-. \tag{6}$$

Any configurational change induced by rising temperatures must cause increases of configurational entropy. Consistent with this constraint, formation of OH^- ions is favoured by high temperatures (Nowak and Behrens, 1995; Shen and

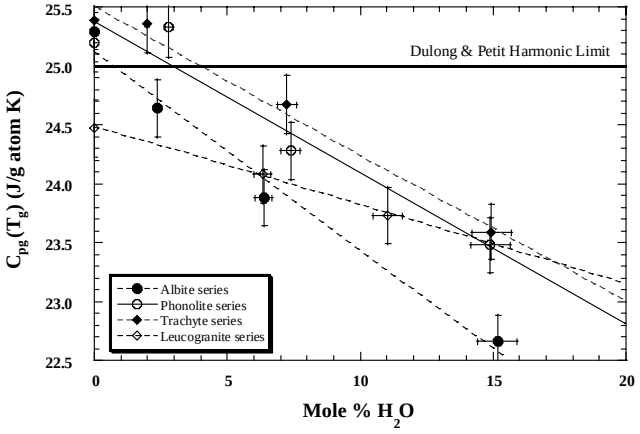

Fig. 7. Heat capacities of the hydrous albite, phonolite, trachyte and DK89 glasses at their glass transition temperatures.

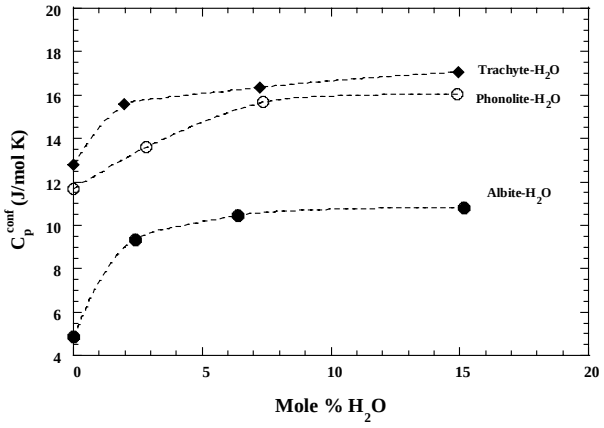

Fig. 8. Configurational heat capacities of the hydrous albite, phonolite and trachyte melts.

Keppler, 1995; Sowerby and Keppler, 1999; Behrens and Nowak, 2003) through mixing of molecular water and hydroxyl ions. Hence, part of the configurational heat capacity of albite, phonolite, and trachyte melts is related to the shift of reaction (6) to the right above the glass transition temperature. As discussed previously (Richet et al., 1996; Whittington et al., 2000, 2004), however, the effects of water on viscosity are much stronger near the glass transition than at superliquidus temperatures even though the disproportionation equilibrium favours the formation of OH^- with increasing temperature. The reason is that the relative contribution of the chemical entropy associated with water speciation to the total configurational entropy is the highest at low temperature.

Different mechanisms have been proposed for dissolution of water in aluminosilicate melts and the role of hydroxyl groups is still a matter of debate (e.g., Kohn, 2000; Mysen and Richet, 2005). However, the NMR study of Robert et al. (2001) on the same hydrated phonolite compositions indicates that at least two dissolution mechanisms may operate simultaneously, as was suggested by Whittington et al. (2001) on the basis of viscosity measurements on the same compositions. The first mechanism involves breaking the strong T–O–T bonds of the aluminosilicate network, and the second may weaken T–O–T bonds by protonation of the bridging oxygen to create a bridging hydroxyl group. NMR spectroscopic studies and ab initio calculations are consistent with both of these dissolution mechanisms also occurring in both albitic and haplogranitic liquids (e.g., Schmidt et al., 2001; Liu et al., 2002), and, by extension, probably also in natural leucogranites such as DK89.

For phonolite and trachyte melts, Whittington et al. (2001) found that addition of water causes very similar viscosity reductions for intermediate compositions with similar NBO/T, irrespective of the identity of the network modifier cations involved (alkali or alkaline earth elements). Similar enthalpies of water exsolution were determined for both phonolitic and trachytic glass series by Richet et al. (2004, 2005), and in the present work, we again find that the thermodynamic parameters investigated are similar for hydrous phonolite and trachyte melts. We therefore conclude that, in this respect, incorporation of water into such melts is not strongly dependent on the nature of the network modifier cations already present.

7. Summary

Our calorimetric experiments indicate that:

(a) The partial molar heat capacity of water in polymerized aluminosilicate glasses and liquids can be considered to be independent of composition, at least for the compositional range of melts studied here.
(b) The effect of water on the decrease of T_g with increasing water content is more pronounced for albite (NBO/$T = 0$), which is the more polymerized melt, than for phonolite (NBO/$T = 0.19$) or trachyte (NBO/$T = 0.21$).
(c) Configurational heat capacity is positively correlated with water content. This increase is essentially due to the fact that the heat capacity of hydrous glasses at the glass transition temperature becomes increasingly smaller than the harmonic limit of $3R$/g atom K with increasing water content.
(d) In agreement with Adam and Gibbs theory, the increase of the configurational heat capacity at the glass transition with water content is consistent with the increasing fragility of the melts revealed by viscosity measurements.
(e) The thermodynamics of water dissolution in substantially polymerized aluminosilicate melts is not strongly dependent on the nature of the network modifier cations already present.

Acknowledgments

This work has been supported by the EU TMR network ERBFMRX 960063 "In situ hydrous melts." The authors thank B.T. Poe, M.J. Toplis, and an anonymous reviewer for their constructive comments. We gratefully thank the Hannover group for help with hydration experiments, T. Withers and H. Behrens for assistance with NIR spectroscopy, and Y. Linard and Ph. Jarry for their help at various stages of this work. M.A. Bouhifd acknowledges the support of NERC through Grant No. NER/A/S/2003/00378.

Associate editor: Brent T. Poe

Appendix A

The C_p experiments for hydrous samples were stopped when anomalous heat effects were observed. In Fig. 9, we show the example for Trach 2.2. The arrow shown in the figure indicates the C_p–temperature data, which terminate the experiment.

See Tables A1–A4.

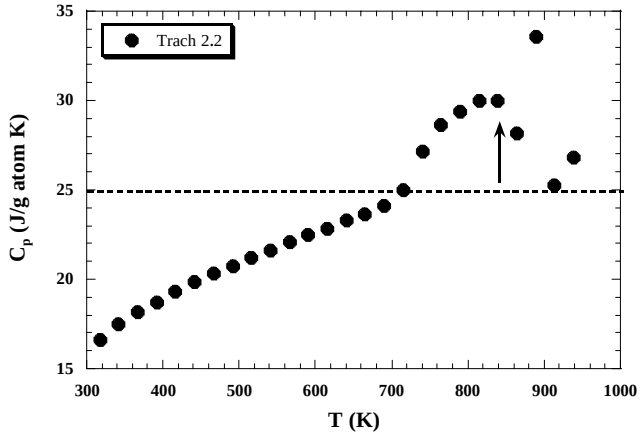

Fig. 9. Heat capacities for Trach 2.2 showing anomalous effects at high temperatures.

Table A1
Experimental heat capacities of the hydrous albite glasses and melts (J/mol K)

Anhydrous albite		HAB 0.6		HAB 2.2		HAB 5.2	
T (K)	C_p	T (K)	C_p	T (K)	C_p	T (K)	C_p
312.7	54.094	316.8	53.526	316.8	53.702	316.9	53.284
337.7	56.111	341.9	56.221	341.9	56.264	341.9	56.131
362.6	58.111	366.7	58.496	366.7	57.683	366.8	58.471
387.4	60.197	391.6	60.118	391.6	60.053	391.6	59.827
412.3	61.684	416.5	62.021	416.5	61.614	416.5	61.604
437.1	63.172	441.3	63.522	441.3	63.324	441.3	63.525
462.0	64.481	466.1	65.087	466.2	64.902	466.2	65.029
486.9	65.934	491.0	66.550	491.0	66.353	491.0	66.810
511.7	66.916	515.9	67.909	515.8	67.962	515.9	68.123
536.6	68.188	540.7	68.933	540.7	69.365	540.7	69.265
561.4	69.265	565.6	70.256	565.5	70.738	565.6	71.518
586.3	70.057	590.4	71.375	590.4	72.083	590.4	74.349
611.1	71.123	615.3	72.435	615.2	73.069	615.3	80.266
636.0	71.677	640.1	73.361	640.1	74.285	640.1	83.378
660.8	72.568	665.0	74.286	664.9	75.874	665.0	84.378
685.6	73.237	689.8	75.099	689.8	79.742	689.8	84.492
710.5	73.845	714.7	75.877	714.7	86.117		
735.3	74.390	739.5	76.920	739.5	87.347		
760.2	74.865	764.4	77.891	764.4	88.400		
785.0	75.624	789.2	79.006	789.2	88.678		
809.9	76.106	814.1	81.559	814.0	89.251		
834.7	76.301	838.9	86.913				
859.5	77.034	863.7	88.749				
884.4	77.624	888.6	90.112				
909.2	78.185	913.4	90.276				
934.0	78.507	938.2	90.887				
958.9	79.104						
983.7	79.425						
1008.5	80.689						
1033.4	81.233						
1058.2	82.726						
1083.0	86.188						

Table A2
Experimental heat capacities of hydrous phonolite glasses and melts (J/mol K)

Phon 0.		Phon 0.5B		Phon 2.2		Phon 5	
T (K)	C_p	T (K)	C_p	T (K)	C_p	T (K)	C_p
316.9	55.410	316.8	52.895	316.8	53.669	316.8	52.981
341.9	57.647	341.8	56.010	341.9	55.629	341.8	55.080
366.7	59.389	366.7	57.284	366.7	58.512	366.7	58.488
391.6	61.092	391.6	60.264	391.6	60.606	391.6	60.523
416.4	62.608	416.4	62.062	416.4	62.336	416.4	62.441
441.3	64.328	441.3	63.478	441.3	64.215	441.3	64.353
466.2	65.778	466.1	65.120	466.2	65.733	466.1	66.211
491.0	67.113	491.0	66.685	491.0	67.167	491.0	67.867
515.9	68.105	515.8	67.660	515.8	68.577	515.8	69.426
540.7	69.244	540.7	69.468	540.7	69.887	540.7	71.358
565.6	70.553	565.5	70.591	565.6	71.120	565.5	74.916
590.4	71.278	590.4	71.529	590.4	72.848	590.4	81.771
615.3	72.166	615.2	72.736	615.2	73.612	615.3	87.454
640.1	73.004	640.1	74.004	640.1	76.142	640.1	90.358
665.0	73.665	664.9	75.071	665.0	78.129	665.0	90.422
689.8	74.191	689.8	76.012	689.8	86.218		
714.7	74.925	714.6	77.089	714.7	91.544		
739.5	75.497	739.5	78.289	739.5	93.181		
764.4	76.250	764.3	79.615	764.4	92.666		

Table A2 (*continued*)

Phon 0.		Phon 0.5B		Phon 2.2		Phon 5	
T (K)	C_p	T (K)	C_p	T (K)	C_p	T (K)	C_p
789.3	77.013	789.2	82.189				
814.1	77.818	814.0	90.509				
839.0	78.521	838.9	93.485				
863.8	79.396	863.7	94.367				
888.7	81.179	888.5	94.497				
913.5	86.279	913.4	94.376				
938.4	91.284						
963.2	92.273						
988.0	92.443						
1012.9	92.232						
1037.7	92.114						
1062.5	92.088						

Table A3
Experimental heat capacities of hydrous trachyte glasses and melts (J/mol K)

Trach 0.		Trach 50		Trach 2.2		Trach 5	
T (K)	C_p	T (K)	C_p	T (K)	C_p	T (K)	C_p
316.9	52.507	316.8	51.057	316.9	51.466	316.9	50.591
341.9	54.864	341.8	54.231	341.9	54.130	341.8	53.217
366.7	56.748	366.7	56.435	366.7	56.255	366.7	55.734
391.6	58.213	391.6	58.370	391.6	57.972	391.6	57.520
416.4	59.659	416.4	59.892	416.5	59.754	416.4	59.458
441.3	61.720	441.3	61.441	441.3	61.412	441.3	61.158
466.2	63.075	466.1	62.995	466.2	62.867	466.1	62.559
491.0	64.477	491.0	64.426	491.0	64.238	491.0	64.271
515.9	65.517	515.8	65.520	515.9	65.601	515.8	65.869
540.7	66.751	540.7	66.890	540.8	66.913	540.7	67.341
565.6	68.165	565.5	68.063	565.6	68.227	565.6	68.924
590.4	68.655	590.4	68.465	590.5	69.486	590.4	71.250
615.3	69.535	615.2	70.439	615.3	70.561	615.3	74.809
640.1	70.278	640.1	70.400	640.2	72.000	640.1	81.068
665.0	70.950	664.9	71.040	665.0	73.112	665.0	84.114
689.8	71.425	689.8	72.761	689.9	74.642	689.8	87.641
714.7	72.161	714.6	73.474	714.7	77.323	714.7	89.785
739.5	72.848	739.5	74.551	739.6	84.077	739.5	89.813
764.4	73.508	764.3	75.492	764.4	88.565		
789.3	74.300	789.2	76.401	789.3	90.901		
814.1	75.015	814.0	77.884	814.2	92.683		
839.0	75.639	838.9	80.108	839.0	92.745		
863.8	76.178	863.7	85.587				
888.7	76.879	888.6	91.539				
913.5	77.690	913.4	93.964				
938.4	79.388	938.2	94.288				
963.2	84.763	963.1	94.394				
988.0	90.010						
1012.9	91.590						
1037.7	91.662						
1062.5	91.527						

Table A4
Experimental heat capacities of the hydrous Leucogranite glasses and melts (J/mol K)

Anhydrous DK89		DK89-1.5		DK89-3	
T (K)	C_p	T (K)	C_p	T (K)	C_p
316.9	52.199	316.8	51.183	316.8	51.347
341.9	55.234	341.8	53.319	341.8	53.946

Table A4 (*continued*)

Anhydrous DK89		DK89-1.5		DK89-3	
T (K)	C_p	T (K)	C_p	T (K)	C_p
366.7	56.826	366.7	55.487	366.7	56.270
391.6	58.473	391.6	57.547	391.5	58.379
416.4	59.716	416.4	59.023	416.4	60.425
441.3	61.570	441.3	61.248	441.3	62.045
466.2	62.751	466.1	62.904	466.1	63.992
491.0	64.208	491.0	64.059	491.0	65.508
515.9	65.423	515.8	65.579	515.8	66.528
540.7	66.338	540.7	66.828	540.7	68.067
565.6	67.719	565.5	67.909	565.5	69.146
590.4	68.399	590.4	69.383	590.4	70.600
615.3	68.997	615.2	70.392	615.2	72.172
640.1	70.019	640.1	71.464	640.1	74.123
665.0	70.817	664.9	72.374	664.9	76.353
689.8	71.172	689.8	73.620	689.8	81.791
714.7	71.759	714.6	74.905	714.6	83.493
739.5	72.270	739.5	77.306		
764.4	73.268	764.3	81.585		
789.3	73.723	789.2	83.431		
814.1	74.221	814.0	84.037		
839.0	74.748				
863.8	75.129				
888.7	75.706				
913.5	76.250				
938.4	77.025				
963.2	79.013				
988.0	83.935				
1012.9	86.262				
1037.7	86.879				
1062.5	87.001				

References

Adam, G., Gibbs, J.H., 1965. On the temperature dependence of cooperative relaxation properties in glass-forming liquids. *J. Chem. Phys.* **43**, 139–146.

Behrens, H., Romano, C., Nowak, M., Holtz, F., Dingwell, D.B., 1996. Near-infrared spectroscopic determination of water species in glasses of the system $MAlSi_3O_8$ (M = Li, Na, K): an interlaboratory study. *Chem. Geol.* **128**, 41–63.

Behrens, H., Nowak, M., 2003. Quantification of H_2O speciation in silicate glasses and melts by IR spectroscopy – *in situ* versus quench techniques. *Phase Transitions* **76**, 45–61.

Bouhifd, M.A., Courtial, P., Richet, P., 1998. Configurational heat capacities: alkali vs. alkaline-earth aluminosilicate liquids. *J. Non-Cryst. Solids* **231**, 169–177.

Bouhifd, M.A., Sipp, A., Richet, P., 1999. Heat capacity, viscosity, and configurational entropy of alkali titanosilicate melts. *Geochim. Cosmochim. Acta* **63**, 2429–2437.

Bouhifd, M.A., Whittington, A., Richet, P., 2001. Partial molar volume of water in phonolitic glasses and liquids. *Contrib. Mineral. Petrol.* **142**, 235–243.

Burnham, C.W., Davis, N.F., 1974. The role of H_2O in silicate melts: II. Thermodynamic and phase relations in the system $NaAlSi_3O_8 \cdot H_2O$ to 10 kilobars, 700–1100 °C. *Am. J. Sci.* **274**, 902–940.

Carroll, M.R., Blank, J.G., 1997. The solubility of H_2O in phonolitic melts. *Am. Mineral.* **82**, 549–556.

Casey, D.N., Hetherington, G., Winterburn, J.A., Yates, B., 1976. The influence of the hydroxyl content upon the specific heat capacity of vitreous silica at elevated temperatures. *Phys. Chem. Glasses* **17**, 77–82.

Clemens, J.D., Navrotsky, A., 1987. Mixing properties of $NaAlSi_3O_8$ melt-H_2O: new calorimetric data and some geological implications. *J. Geol.* **95**, 173–186.

Courtial, P., Richet, P., 1993. Heat capacity of magnesium aluminosilicate melts. *Geochim. Cosmochim. Acta* **57**, 1267–1275.

Davis, M.J., 1998. The effect of water on the viscosity of silicate melts: a configurational entropy approach. *Geochim. Cosmochim. Acta* **63**, 167–173.

Dingwell, D.B., Romano, C., Hess, K.U., 1996. The effect of water on the viscosity of a haplogranitic melt under P–T–X conditions relevant to silicic volcanism. *Contrib. Mineral. Petrol.* **124**, 19–28.

Haggerty, J.S., Cooper, A.R., Heasley, J.H., 1968. Heat capacity of three inorganic glasses and liquids and supercooled liquids. *Phys. Chem. Glasses* **9**, 47–51.

Kohn, S.C., 2000. The dissolution mechanisms of water in silicate melts; a synthesis of recent data. *Mineral. Mag.* **64**, 389–408.

Lange, A.R., Navrotsky, A., 1993. Heat capacities of TiO_2-bearing silicate liquids: evidence for anomalous changes in configurational entropy with temperature. *Geochim. Cosmochim. Acta* **57**, 3001–3011.

Linard, Y., 2000. Détermination des enthalpies libres de formation des verres borosilicatés. PhD thesis, Université Paris 7, 265 pp.

Linard, Y., Yamashita, I., Atake, T., Rogez, J., Richet, P., 2001. Thermochemistry of nuclear waste glasses: an experimental determination. *J. Non-Cryst. Solids* **286**, 200–209.

Liu, Y., Nekvasil, H., Long, H., 2002. Water dissolution in albite melts: constraints from ab initio NMR calculations. *Geochim. Cosmochim. Acta* **66**, 4149–4163.

Maschmeyer, R.O., 1980. Hydrosilicates: hydration thermodynamics. *J. Non-Cryst. Solids* **38-39**, 655–660.

Moynihan, C.T., 1995. Structural relaxation and the glass transition. *Rev. Mineral.* **32**, 1–19.

Mysen, B.O., Richet, P., 2005. *Silicate Glasses and Melts: Properties and Structure*. Elsevier, Amsterdam.

Nowak, M., Behrens, H., 1995. The speciation of water in haplogranitic glasses and melts determined by in-situ near-infrared spectroscopy. *Geochim. Cosmochim. Acta* **59**, 3445–3450.

Ochs, F.A., Lange, R.A., 1999. The density of hydrous magmatic liquids. *Science* **283**, 1314–1317.

Richet, P., 1984. Viscosity and configurational entropy of silicate melts. *Geochim. Cosmochim. Acta* **48**, 471–483.

Richet, P., 1987. Heat capacity of silicate glasses. *Chem. Geol.* **62**, 111–124.

Richet, P., Bottinga, Y., 1984. Glass transitions and thermodynamic properties of amorphous SiO_2, $NaAlSi_nO_{2n+2}$ and $KAlSi_3O_8$. *Geochim. Cosmochim. Acta* **48**, 453–470.

Richet, P., Bottinga, Y., 1985. Heat capacity of aluminium-free liquid silicates. *Geochim. Cosmochim. Acta* **49**, 471–486.

Richet, P., Bottinga, Y., 1986. Thermochemical properties of silicate glasses and liquids: a review. *Rev. Geophys.* **24**, 1–25.

Richet, P., Polian, A., 1998. Water as a dense icelike component in silicate glasses. *Science* **281**, 396–398.

Richet, P., Lejeune, A.M., Holtz, F., Roux, J., 1996. Water and the viscosity of andesite melts. *Chem. Geol.* **128**, 185–197.

Richet, P., Bouhifd, M.A., Courtial, P., Téqui, C., 1997. Configurational heat capacity and entropy of borosilicate melts. *J. Non-Cryst. Solids* **211**, 271–280.

Richet, P., Whittington, A., Holtz, F., Behrens, H., Ohlhorst, S., Wilke, M., 2000. Water and the density of silicate glasses. *Contrib. Mineral. Petrol.* **138**, 337–347.

Richet, P., Hovis, G.L., Whittington, A., Roux, J., 2004. Energetics of water dissolution in trachyte glasses and liquids. *Geochim. Cosmochim. Acta* **68**, 5151–5158.

Richet, P., Hovis, G.L., Whittington, A., 2005. Water and magmas: thermal effects of water exsolution. *Earth Planet. Sci. Lett.*, in press.

Robert, E., Whittington, A., Fayon, F., Pichavant, M., Massiot, D., 2001. Structural characterization of water bearing silicate and aluminosilicate glasses by high resolution solid state NMR. *Chem. Geol.* **174**, 291–305.

Romano, C., Poe, B., Mincione, V., Hess, K.U., Dingwell, D.B., 2001. The viscosities of dry and hydrous $XAlSi_3O_8$ (X = Li, Na, K, $Ca_{0.5}$, $Mg_{0.5}$) melts. *Chem. Geol.* **174**, 115–132.

Romano, C., Giordano, D., Papale, P., Mincione, V., Dingwell, D.B., Rosi, M., 2003. The dry and hydrous viscosities of alkaline melts from Vesuvius and Phlegrean fields. *Chem. Geol.* **202**, 23–38.

Schairer, J.F., Bowen, N.L., 1955. The system K_2O–Al_2O_3- SiO_2. *Am. J. Sci.* **253**, 681–746.

Schmidt, B.C., Riemer, T., Kohn, S.C., Holtz, F., Dupree, R., 2001. Structural implications of water dissolution in haplogranitic glasses from NMR spectroscopy: influence of total water content and mixed alkali effect. *Geochim. Cosmochim. Acta* **65**, 2949–2964.

Shen, A., Keppler, H., 1995. Infrared spectroscopy of hydrous silicate melts to 1000 °C and 10 kbar—direct observation of H_2O speciation in a diamond-anvil cell. *Am. Mineral.* **80**, 1335–1338.

Silver, L.A., Stolper, E., 1989. Water in albitic glasses. *J. Petrol.* **30**, 667–709.

Silver, L.A., Ihinger, P.D., Stolper, E., 1990. The influence of bulk composition on the speciation of water in silicate glasses. *Contrib. Mineral. Petrol.* **104**, 142–162.

Sipp, A., Richet, P., 2002. Equivalence of volume, enthalpy and viscosity relaxation kinetics in glass-forming silicate liquids. *J. Non-Cryst. Solids* **298**, 202–212.

Sowerby, J.R., Keppler, H., 1999. Water speciation in rhyolitic melt determined by in-situ infrared spectroscopy. *Am. Mineral.* **84**, 1843–1849.

Stebbins, J.F., Xu, Z., 1997. NMR evidence for excess non-bridging oxygen in an aluminosilicate glass. *Nature* **390**, 60–62.

Stolper, E., 1982. Water in silicate glasses: an infrared spectroscopic study. *Contrib. Mineral. Petrol.* **81**, 1–17.

Tangeman, J.A., Lange, R.A., 1998. The effect of Al^{3+}, Fe^{3+}, and Ti^{4+} on the configurational heat capacities of sodium silicate liquids. *Phys. Chem. Minerals* **26**, 83–99.

Toplis, M.J., Dingwell, D.B., Lenci, T., 1997. Peraluminous viscosity maxima in Na_2O–Al_2O_3–SiO_2 liquids: the role of triclusters in tectosilicate melts. *Geochim. Cosmochim. Acta* **61**, 2605–2612.

Toplis, M.J., Kohn, S.C., Smith, M.E., Poplett, I.J.F., 2000. Fivefold-coordinated aluminium in tectosilicate glasses observed by triple quantum MAS NMR. *Am. Mineral.* **85**, 1556–1560.

Toplis, M.J., Gottsmann, J., Knoche, R., Dingwell, D.B., 2001. Heat capacities of haplogranitic glasses and liquids. *Geochim. Cosmochim. Acta* **65**, 1985–1994.

Webb, S.L., Knoche, R., 1996. The glass transition, structural relaxation and shear viscosity of silicate melts. *Chem. Geol.* **128**, 165–183.

Whittington, A., Richet, P., Holtz, F., 2000. Water and the viscosity of depolymerized aluminosilicate melts. *Geochim. Cosmochim. Acta* **64**, 3725–3736.

Whittington, A., Richet, P., Linard, Y., Holtz, F., 2001. The viscosity of hydrous phonolites and trachytes. *Chem. Geol.* **174**, 209–223.

Whittington, A., Richet, P., Behrens, H., Holtz, F., Scaillet, B., 2004. Experimental temperature-X(H_2O)-viscosity relationship of leucogranites, and comparison with synthetic silicic liquids. *Trans. Roy. Soc. Edin.: Earth Sci.* **95**, 59–72.